

**FIGURE 7.20**

Schematic of the Tomsk system for driving a magnetron with a linear induction accelerator: (1) ferromagnetic core, (2) magnetizing turn, (3) strip DFL, (4) housing, (5) cathode, (6) helical winding, (7) insulator, (8) protecting shield, (9) magnet system, (10) shunt for operating current of the magnetron, (11) anode unit of the relativistic magnetron, (12) drift tube, (13) cathode, (14) antenna for outlet of microwave radiation, (15) terminal for demagnetizing, (16) total current Rogowski loop, (17) multichannel discharge, and (18) input of high voltage for the DFL charge. (From Vasil'yev, V.V. et al., *Sov. Tech. Phys. Lett.*, 13, 762, 1987. With permission.)

replaced at 1000 to 1500 shots, and the spark gaps in the pulsed power had to be cleaned after 2000 to 5000 shots.

Compact linear induction accelerators developed at the Scientific-Research Institute of Nuclear Physics of the Tomsk Polytechnic Institute in Russia<sup>38</sup> and refined at Physics International (now L-3 Communications Pulse Sciences) in the U.S.<sup>39</sup> provide the necessary power at repetition rates that have been pushed to 1000 Hz in five-pulse bursts (limited by the stored energy available). The system is compact because high voltage is generated by inductively adding relatively lower voltages along a coaxial line; peak voltage, with its volume and mass demands, appears only on the load. Longer lifetime is provided by using magnetic, rather than spark-gap, switches operating at lower voltages. The Tomsk system is shown schematically in Figure 7.20<sup>38</sup>; a photo of the device in Figure 7.21 shows that it is quite compact. The repetition rate is 50 Hz, generating a peak microwave power of 360 MW in the magnetron from a 4-kA, 300-kV, 60-nsec electrical pulse. The ability to operate at higher rates was proven by a three-pulse burst at 160 Hz, achieved by firing during the flat period of the pulsed magnetic field coil. The average power was reported to be about 1 kW.

Five years after the first Tomsk publication, the Physics International group built CLIA (Compact Linear Induction Accelerator) to drive a six-vane, 1.1-GHz magnetron<sup>16</sup>; a 100-nsec version of CLIA without a magnetron is shown in Figure 7.22. The L-band magnetron had produced 3.6 GW in single pulses with a Marx bank/waterline driver, but power was reduced on CLIA due to the mismatch of the 25- $\Omega$  magnetron to the 75- $\Omega$  output impedance of the driver. The magnetron was modified with the addition of cooling channels

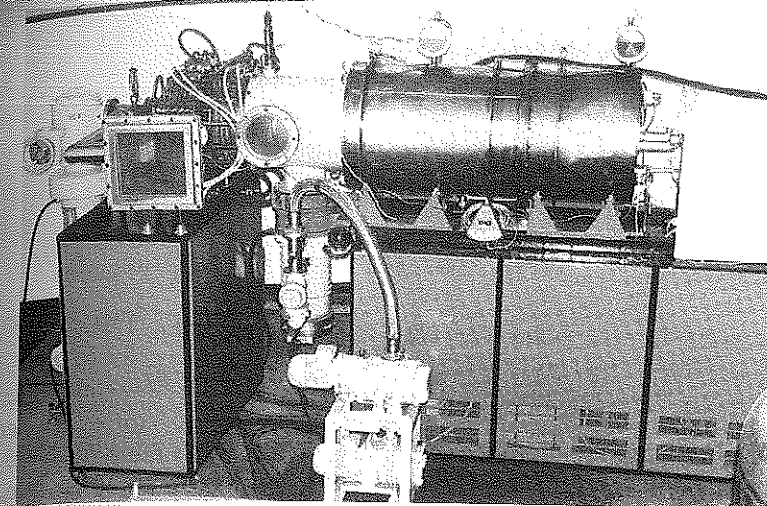


**FIGURE 7.21**

The Tomsk linear induction accelerator and magnetron system.

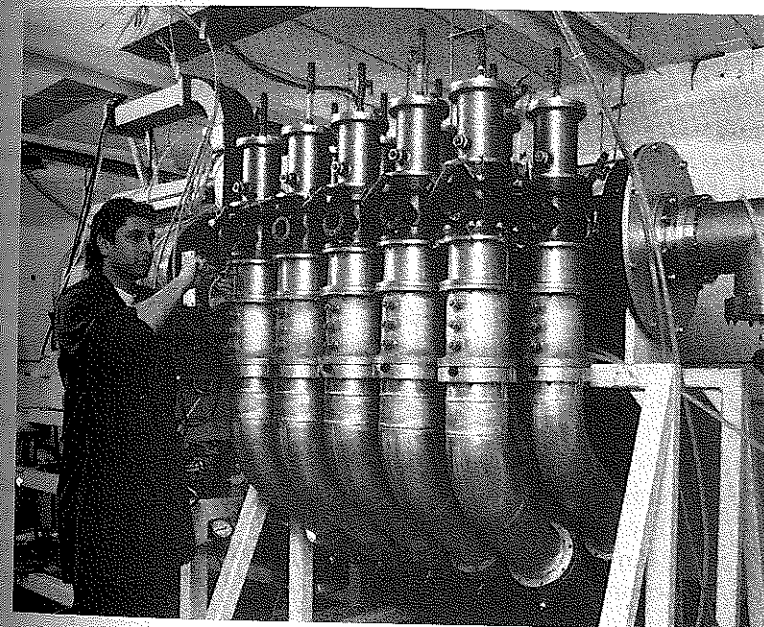


**FIGURE 7.22**

Inductive adder with 10 pulse-forming lines for the 100-nsec Compact Linear Induction Accelerator. (Courtesy of David Price, L-3 Communications Pulse Sciences.)

TABLE 7.5

Summary of Magnetron Peak and Average Power Performance on the Compact Linear Induction Accelerator (CLIA)

Repetition Rate (Hz)	Peak Power (MW)	Average Power (kW)	Number of Shots
100	1000	4.4	50
200	700	6.0	100
250	600	6.3	100
1000 <sup>a</sup>	600	25	5

<sup>a</sup> Based on the third shot in a five-shot sequence.

3 mm below the surface and a cryopump to eliminate possible contamination with backstreaming pump oil (base pressure was  $4 \times 10^{-6}$  torr). The performance at four different repetition rates is summarized in Table 7.5. Note that even though the peak power declined with increasing repetition rate, the average power climbed. Note also that even though the 1000-Hz burst was limited to five shots, this repetition rate far exceeded the average-current capability of the system. Pulse-to-pulse reproducibility on this system was remarkable, as was the fact that there was no pulse shortening in this lower-frequency, larger magnetron ( $r_c$  and  $r_a$  of 1.27 and 3.18 cm vs. 1.3 and 2.1 in the 2.3-GHz  $\pi$ -mode of the A6).

The L-band magnetron also illustrates another empirical observation: anode erosion appears to worsen with increasing frequency, probably due to the reduced anode dimensions and roughly constant electrical current. There was no noticeable erosion on the larger, lower-frequency L-band magnetron after several hundred shots on single-shot generators and several thousand on CLIA; erosion was noticeable on the 4.6-GHz magnetron of Spang et al.<sup>34</sup> after 5000 shots, although performance was unimpaired at that point; and erosion was severe in the X-band magnetrons of Kovalev et al.<sup>15</sup> and Benford and Sze.<sup>31</sup>

#### 7.4.4 Magnetron-Based Testing Systems: MTD-1 and Orion

From the standpoints of size and flexibility, the Mobile Test Device-1 (MTD-1) of AAI<sup>34</sup> and the Orion transportable test facility of Physics International<sup>40</sup> represent the two extremes of magnetron-based testing systems. MTD-1 was designed to minimize size and weight; the core of the system is depicted in Figure 7.23.<sup>34</sup> The pulsed power and 700-MW, A6 variant magnetron fit in a  $182 \times 91 \times 182$  cm<sup>3</sup> package, and the auxiliary controls, high-voltage power supplies, and connector panel fit within another  $61 \times 71 \times 152$  cm<sup>3</sup> volume. The mass of the system, including heat exchanger and prime power, was 1500 kg, and with a trailer the total was 2200 kg. Power could be radiated from a horn antenna, a lens antenna with a 23-dB gain, or a dielectric rod antenna with a 32-dB gain.

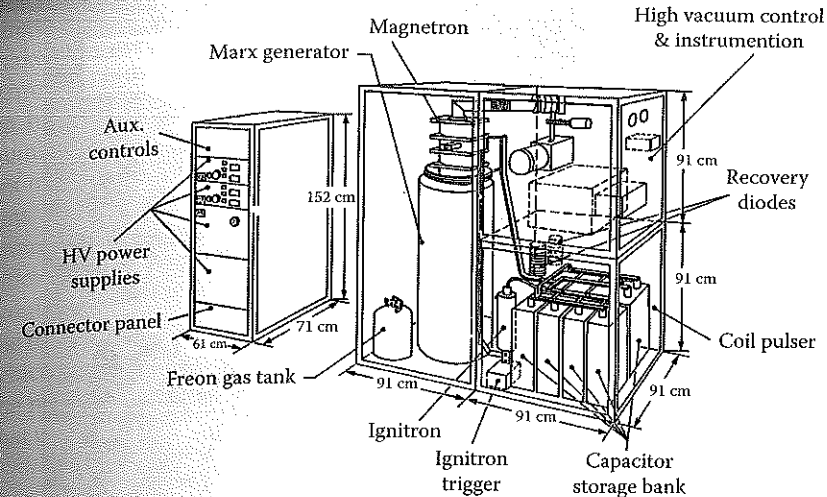


FIGURE 7.23

Diagram of the Mobile Test Device-1 (MTD-1) from AAI Corporation. (From Spang, S.T. et al., *IEEE Trans. Plasma Sci.*, PS-18, 586, 1990. With permission.)

Orion, also described in Section 5.7, was designed to provide a full, transportable microwave effects field testing facility in five ISO containers: (1) prime power, including station keeping, and air conditioning; (2) a source container, connected at right angles to the (3) operations container; (4) a control container; and (5) a storage container. The layout of all but the storage container in a testing configuration is shown in Figure 7.24.<sup>40</sup> The pulse length of the output from the pulsed power system is adjustable in 50-nsec increments between 100 and 500 nsec, with reduced voltage output at the longer pulse length. At the heart of the system, the insertion of one of four mechanically tunable rising-sun magnetrons allows the system to cover the frequency range from 1 to 3 GHz. Each magnetron produces 400 to 800 MW of output power and can be fired repetitively at a rate of 100 Hz in a 1000-pulse burst. Microwaves are radiated from a parabolic antenna that illuminates a  $7 \times 15$  m<sup>2</sup>, 3-dB elliptical spot at a 100-m range, and a waveguide combiner/attenuator allows the power to the antenna to be varied over five orders of magnitude.

#### 7.5 Research and Development Issues

The key operational parameters for a relativistic magnetron are:

- Peak power
- Efficiency



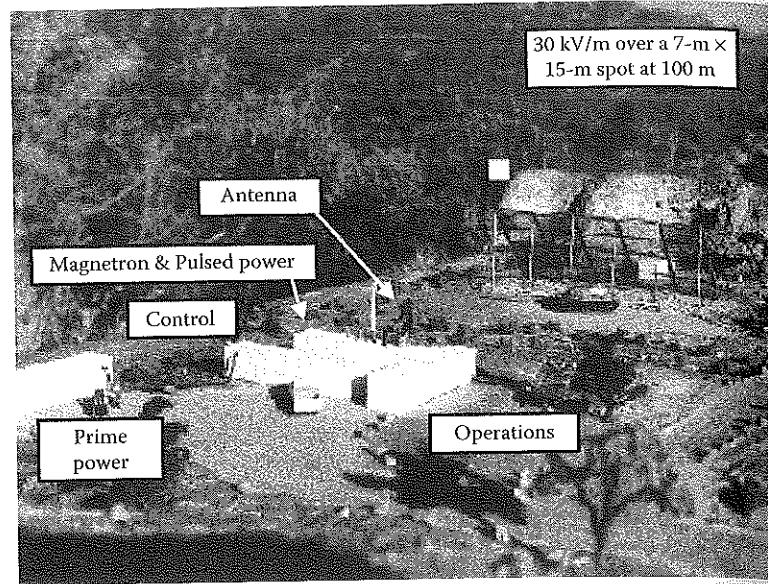


FIGURE 7.24

The Orion system in the field (storage container not shown). The truck in front of the control container provides a sense of scale. (Courtesy of L-3 Communications Pulse Sciences.)

- Pulse duration or energy per pulse
- Pulse repetition rate or average power
- Magnetron lifetime

Within this set, the area of most active research and development is that of pulse duration or, as it is most commonly referred to, *pulse shortening*, stemming from the common observation in all high power microwave (HPM) sources that at the highest power levels, the microwave output pulse is shorter than that of the current and voltage pulses to the magnetron. Further, as the output power increases, the pulse duration decreases.

The issues underlying the *achievable pulse repetition rate* are a combination of physics issues in the source and technological constraints in the prime and pulsed power. In the case of the physics issues, the phenomena are similar to those involved in pulse shortening: plasma is evolved from the electrodes that must then be cleared before the next shot can be fired. On the other hand, an example of a technological constraint is the amount of prime power available, a limitation imposed by either the power feed to a facility or, for a mobile system, volume and mass. A second constraint is the achievable repetition rate of the pulsed power output switch at the required voltage and current.

Maximizing *power* and *efficiency* has also been an active area of research in the past, as has the issue of magnetron *lifetime*. Power, efficiency, and lifetime are clearly interrelated. Maximizing efficiency for a given power helps to

lengthen lifetime, since as more energy is extracted from the electrons to make microwaves, less is deposited in the anode, reducing heating and damage. High efficiencies also reduce the demand on the prime power and on high-stress pulsed power components. As we can see in Table 7.2, a number of groups have operated individual relativistic magnetrons at powers of several gigawatts in both the  $\pi$ - and  $2\pi$ -modes. Efficiencies of some tens of percent in the L- and S-bands have been achieved, with a peak of around 40%. The issues underlying the maximization of peak power and efficiency are a combination of fundamental limitations and open issues that would profit from further research. We defer to Section 7.6 a discussion of the role of fundamentally limiting values for the electric and magnetic fields, which are relatively well understood, as is the scaling with frequency and the need to limit axial current loss. On the other hand, two research issues that we will discuss here are phase locking of multiple sources and extraction.

### 7.5.1 Pulse Shortening

Unfortunately, progress achieved in radiating higher peak power levels in all classes of HPM sources has been tempered by the pulse-shortening problem.<sup>41</sup> The phenomenon in the case at hand, relativistic magnetrons, is shown in Figure 7.25.<sup>42</sup> The microwave power falls with frequency as  $P \sim f^2$  and with pulse length  $\tau$  as  $P \sim \tau^{-5/3}$ . This limits radiated energies to a few hundred joules. The implication is clear: to get longer pulses, one must accept less energy per pulse.

Why does pulse shortening matter? Consistent with our earlier notation, let  $\eta$  be the power efficiency, the ratio of instantaneous microwave power  $P$

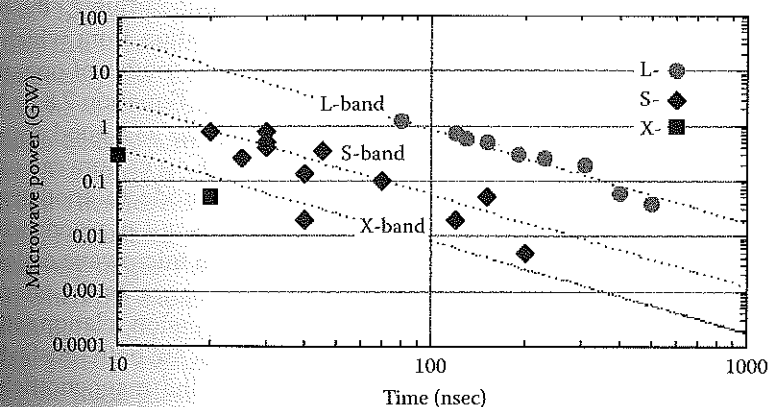


FIGURE 7.25

Pulse length in relativistic magnetrons with explosive emission cathodes decreases as the peak output power increases. Data are from magnetron experiments conducted over the past two decades. All scaling curves are normalized to the L-band, 80 nsec, 1.2-GW point. (From Price, D. et al., *IEEE Trans. Plasma Sci.*, 26, 348, 1998. With permission.)

to electrical pulsed power input  $P_{pp} = VI$ , and  $\eta_E$  be the energy efficiency, the ratio of microwave energy in the pulse  $E$  to the pulsed power electrical energy that drives the beam,  $E_{pp}$ . Then, with  $\tau$  the pulse duration of microwaves and  $\tau_{pp}$  the pulse duration of the pulsed power voltage and current to the magnetron, the relations are

$$E = P\tau \quad (7.16)$$

$$E_{pp} = P_{pp}\tau_{pp} \quad (7.17)$$

Therefore,

$$\frac{\eta_E}{\eta} = \frac{\tau}{\tau_{pp}} \quad (7.18)$$

where  $\tau/\tau_{pp}$  is the pulse-shortening ratio of the energy efficiency to the power efficiency. Today, high values for the magnetron are  $\eta \sim 20$  to 40%, but pulse shortening makes  $\eta_E < 10\%$ . Returning to a point made in Section 7.4.3, the HPM system designer is concerned with the energy that must be supplied by the prime power and stored in pulsed power because energy drives HPM system volume and mass. Therefore,  $\eta_E$  is frequently more meaningful than  $\eta$ ; the distinction between them is the pulse-shortening ratio.

Models to account for pulse shortening in relativistic magnetrons focus on the radial motion of the cathode plasma. The dense, conducting cathode plasma shields the actual cathode and makes the effective cathode radius a time-varying quantity dependent on the radial motion of the plasma surface,  $r_c(t)$ . Recall that the following all depend on the cathode radius,  $r_c$ : the Hull insulation condition (Equation 7.5), the dispersion relation from which we determine the frequencies of the magnetron's different modes of operation (see Section 4.4.2), and the Buneman-Hartree relation (Equation 7.8 or 7.9), which bounds the operating space in  $V$ - $B_z$  space and acts as a good approximation for the operating values of these parameters. Gap closure can cause frequency hopping, as the system jumps from one mode to another; the termination of the microwave pulse as the system falls out of resonance; or the remarkable behavior seen in Figure 7.26,<sup>42</sup> in which microwave emission begins when the system dynamically slips into resonance as the effective cathode radius,  $r_c(t)$ , reaches a value at which the dispersion relation setting the mode frequency and the Buneman-Hartree relation are both satisfied for the given voltage and magnetic field. Note that as the magnetic field is increased in the figure, the microwave pulse turns on later and later in the voltage pulse (and typically terminates before the end of the voltage pulse). While difficult to quantify, we can show that this behavior is consistent with the Buneman-Hartree relation, which we recount from Equation 7.8, making use of Equation 7.7:

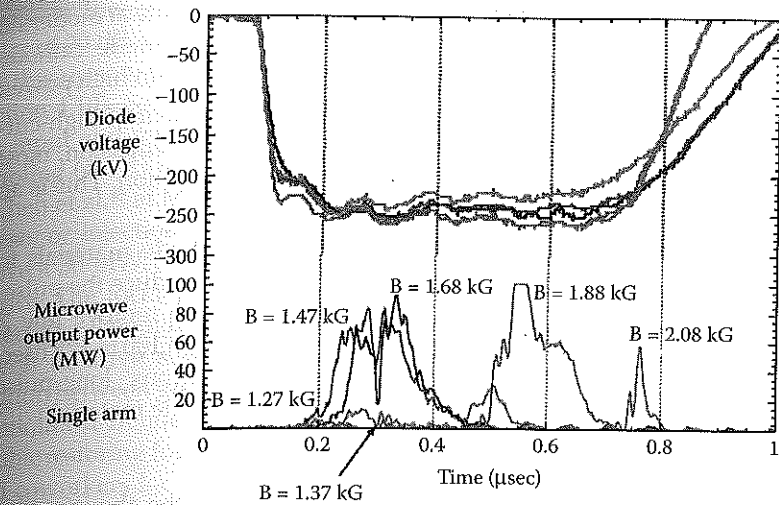


FIGURE 7.26

Observed microwave output pulses for different values of the applied magnetic field (lower curves) and the corresponding voltage pulses on a relativistic magnetron. Modes appearing well below 1.58 kG, at 1.27 and 1.37 kG, are not the fundamental  $\pi$ -mode. (From Price, D. et al., *IEEE Trans. Plasma Sci.*, 26, 348, 1998. With permission.)

$$\frac{eV}{mc^2} = \frac{eB_z\omega_n}{2mc^2n} \left( r_a^2 - r_c^2 \right) - 1 + \sqrt{1 - \left( \frac{r_a\omega_n}{cn} \right)^2} \quad (7.19)$$

In the figure, we focus on the magnetic field values above the two lowest, 1.27 and 1.37 kG, since at those two field values, the magnetron apparently operates in a mode other than the  $\pi$ -mode. At all higher fields, we know that the frequency for the  $\pi$ -mode in which the magnetron operates is quite insensitive to the cathode radius; at cathode radii appropriate to the magnetron in question, the  $\pi$ -mode frequency drops from 1.207 to 1.199 GHz, a difference of only 8 MHz, when the cathode radius increases from 1.778 to 2.078 cm. Therefore, if we assume that  $\omega_n = \omega_\pi$  is constant, then the product  $B_z(r_a^2 - r_c^2)$  must be constant from one shot to the next as well. Thus, for successively larger values of  $B_z$ , Equation 7.19 is satisfied at later and later times, when the expanding cathode plasma makes  $r_c$  large enough that the product  $B_z(r_a^2 - r_c^2)$  reaches the approximately constant value. Based on the cathode plasma expansion rate inferred from an analysis of the data in the figure, the main plasma ion constituent was inferred to be hydrogen.

The model of expanding cathode plasma suggests three approaches to extending the microwave pulse duration:

- Reduce the plasma temperature by decreasing the cathode current density that heats the plasma. To do this, designers can produce



either large devices with large cathode areas that operate at moderate impedance or higher-impedance designs with larger anode-cathode gaps that require high voltage (>1 MV) in order to obtain high power.

- Eliminate the plasma, which requires the development of high-current-density cathodes that do not rely on explosive emission, most likely field emission cathodes without plasma formation. This is an active research topic.
- Increase the plasma ion mass, using heavier cathode materials to increase pulse energy. A magnetron experiment to reduce the pulse-shortening mechanism by heating the resonator to remove low Z contaminants successfully lengthened the pulse from 100 to 175 nsec. A substantial improvement in the Orion magnetrons' long-pulse performance was achieved with carbon-fiber cathode material with cesium iodide surface coating.<sup>43</sup>

Efforts are continuing to eliminate pulse shortening by the above methods.

Just as the changing gap spacing can terminate a pulse, the time-changing voltage provided by pulsed power machines can be problematic. A voltage flatness requirement can be obtained from Figure 7.13, the tuning curve. In scans of the magnetic field at fixed voltage, as is typically done in experiments, a  $\Delta B/B$  bandwidth of  $\pm 10\%$  or greater is observed. A comparable bandwidth in voltage at a fixed magnetic field is therefore expected. Treado showed that a lack of voltage flatness truncated the microwave pulse in a long-pulse modulator experiment.<sup>14,44</sup> For conventional magnetrons with their much higher impedances, the voltage flatness requirement is a major determinant of the modulator design. The same is likely to occur in relativistic magnetrons as the field matures.

To summarize, evidence indicates that the magnetron pulse duration is determined by gap closure — as confirmed by the remarkable data in Figure 7.26, which shows a magnetron sliding into resonance at different magnetic fields — and the flatness, or lack of flatness, in the voltage pulse. Changes in either the gap or the voltage can take a magnetron out of resonance and terminate a pulse even before the electrical impedance of the device collapses, as has been observed.

### 7.5.2 Peak Power: Phase-Locking Multiple Sources and Transparent-Cathode Magnetrons

Although the compactness of magnetrons and CFAs is desirable from a packaging standpoint, it becomes a liability as the power, and power density, grows, with gap closure and anode erosion increasingly problematic, particularly at higher frequencies. An obvious solution is to employ multiple sources, either in a master oscillator/power amplifier array with amplifiers such as CFAs or in a phase-locked array of oscillators such as magnetrons. The problems with the former are the lack of a high power CFA and the

relatively low gain demonstrated by conventional CFAs, typically of the order of 20 dB, which necessitates the use of a high power master oscillator. For this reason, the focus to date has been phase locking of magnetrons (see Section 4.10), both in the weak-coupling [ $\rho = (P_i/P_o)^{1/2} \ll 1$ , with  $P_i$  and  $P_o$  the input and output powers for the magnetron being locked] and strong-coupling ( $\rho \sim 1$ ) regimes.

Chen et al.<sup>45</sup> at MIT and Treado et al.<sup>23</sup> at Varian (now CPI) have explored phase, or injection, locking in the weak-coupling regime. The MIT group drove a 30-MW, 300-nsec relativistic magnetron with a 1-MW conventional device. The locking time was rather long because  $\rho$  and locking time are inversely related; however, it does potentially allow one conventional magnetron to drive several relativistic magnetrons, producing a fixed phase relation between groups of high power devices. Chen also studied the effects of nonlinear frequency shift in magnetrons by adding a Duffing term (with a cubic restoring force) to the van der Pol treatment of phase locking.<sup>46</sup> Treado and coworkers locked a 60-MW magnetron based on conventional technology to a 3-MW magnetron.<sup>23</sup>

The Physics International team explored the strong-coupling regime, connecting several magnetrons directly through short waveguides, as shown in Figure 7.27.<sup>47</sup> Operation in this regime minimizes locking time and facilitates phase locking of oscillators with larger natural frequency differences. This latter allows tolerance for oscillator differences in an array.<sup>48</sup> Calculations predict locking in nanoseconds. In experiments with  $\rho = 0.6$ , phase locking at 1.5 GW occurred in about 10 nsec, as shown in the phase discriminator output in Figure 7.28.<sup>47</sup> Because the phase difference is reproducible from shot to shot, this is an example of phase locking, not merely frequency locking. This is a very practical feature: phase adjustments in the feed of an array to correct for shot-to-shot variations in phase differences would not be possible. The experiments used a second diagnostic to demonstrate locking. Pulses from the two magnetrons were radiated from two antennas onto power density diagnostics in an anechoic room, and a fourfold increase in power density (relative to that of a single magnetron) was observed.

Woo et al.<sup>48</sup> derived a requirement on the length of the waveguide connecting the oscillators:

$$\Delta\omega \leq 2\omega\rho |\cos \omega\tau_c| / Q \quad (7.20)$$

where  $\tau_c$  is the transit time of the wave in the connecting guide. This relation is an extension of the Adler condition. For  $\omega\tau_c = n\pi/2$  with  $n$  odd, phase locking cannot occur. Thus, some connecting lengths prevent phase locking. Phase difference can occur in two modes, with a phase difference of either 0 or  $\pi$  between two oscillators. In the experiments of Benford et al.,<sup>47</sup> the latter case is observed (Figure 7.28).

The Physics International group also studied different geometries for phase-locked arrays.<sup>49</sup> They found that the best geometry uses maximum connectivity (Figure 7.29). Calculated locking time for these arrays appears

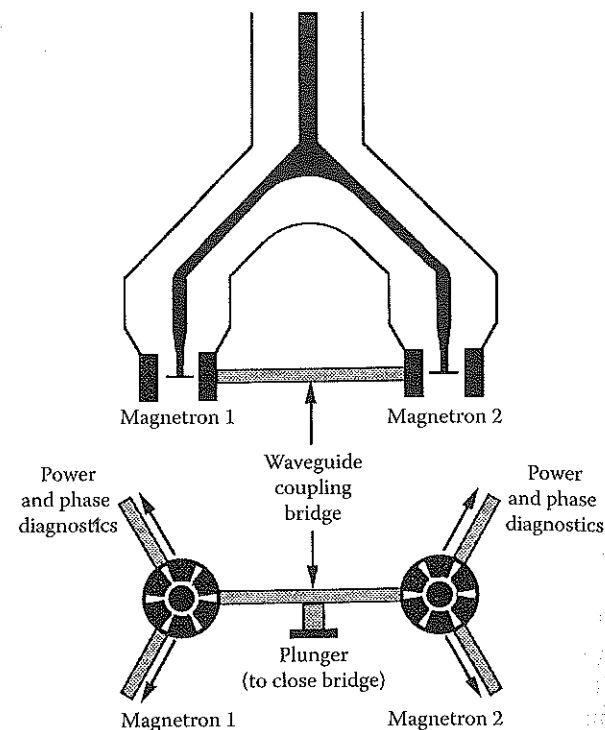


**FIGURE 7.27**  
Two-magnetron phase-locking experiment. (From Benford, J. et al., *Phys. Rev. Lett.*, 62, 969, 1989. With permission.)

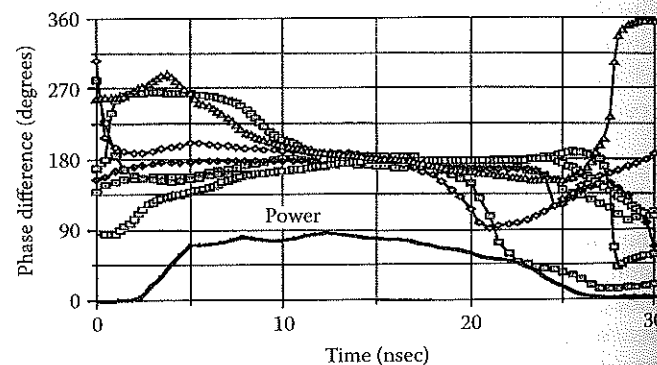


**FIGURE 7.28**  
Phase difference for seven consecutive shots of the two-magnetron experiment. The power pulse shape is shown at the bottom. (From Benford, J. et al., *Phys. Rev. Lett.*, 62, 969, 1989. With permission.)

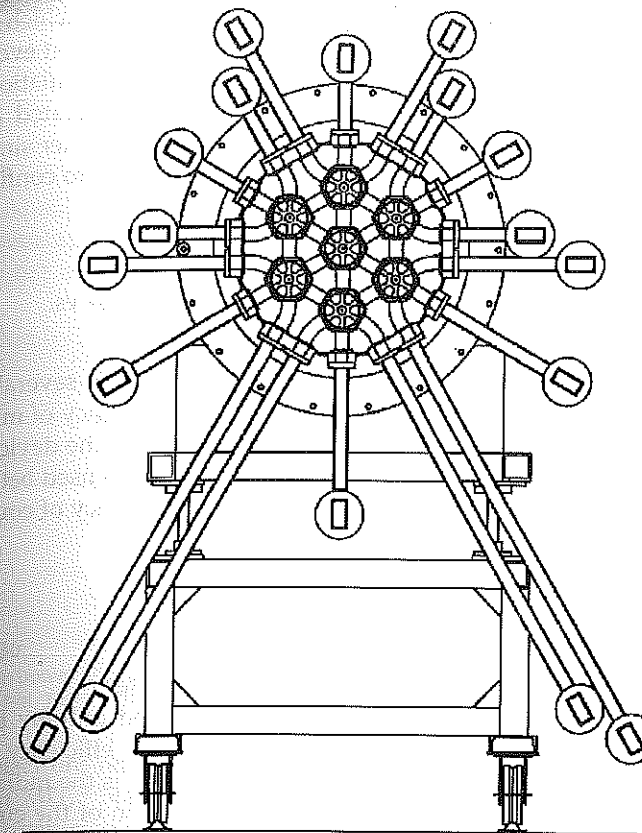


**FIGURE 7.29**  
Seven-magnetron module at Physics International, now L-3 Communications Pulse Sciences. The configuration shown produced the best phase locking among all possibilities considered. (From Levine, J. et al., *Proc. SPIE*, 1226, 60, 1990. With permission.)

to be about that of the two-magnetron experiment. Phase locking was achieved in a seven-magnetron array producing a total output of 3 GW.

Fuks and Schamiloglu have proposed a completely different approach to improving the power and efficiency of magnetrons, the so-called *transparent-cathode magnetron*, in which the solid cathode is replaced by a set of parallel, axial rods, arrayed with equal azimuthal spacing at the radius of a normal cathode.<sup>50</sup> This cathode eliminates the usual boundary condition that the azimuthal component of the RF electric field vanish at the cathode. Thus, the magnitude of the azimuthal electric field component can be larger, which leads to stronger spoke formation, higher power, and higher efficiency. Comparison of simulation results for two versions of the A6 magnetron, one with a solid cathode and the other with a cut cathode consisting of 18 axial rods, shows that while the solid-cathode version produces higher power in the  $2\pi$ -mode at an operating voltage of 350 kV (0.97 vs. 0.55 GW), the efficiency of the transparent-cathode version is significantly higher (25.5 vs. 15%)

because of the higher current of the solid-cathode version, which has four times the cathode surface area of the new version. Operating at even higher voltages (and an appropriately increased magnetic field), simulations of the transparent-cathode magnetron indicate that it can be operated in the  $\pi$ -mode at 1.5 MV and produce over 9 GW. Because the computer simulations are 2-dimensional, experiments will have to be performed to confirm these encouraging results.

### 7.5.3 Efficiency: Limiting Axial Current Loss and Radial vs. Axial Extraction

The efficiency we defined in Equation 7.11 in fact combines several efficiencies, all of which are multiplicative in effect: (1) the efficiency of microwave generation,  $\eta_\mu$ ; (2) the efficiency of power extraction from the device,  $\eta_{ex}$ ; (3) the mode conversion efficiency,  $\eta_{mc}$ , if a mode converter is used between the magnetron and the antenna; and (4) the combined efficiency of coupling to, and radiating from, the antenna,  $\eta_a$ . Therefore,

$$\eta = \eta_\mu \eta_{ex} \eta_{mc} \eta_a \quad (7.21)$$

where we set  $\eta_{mc} = 1$  in the absence of a mode converter.

Consider  $\eta_\mu$  first. Because microwaves are generated only by the radial component of the current, axial current loss reduces the efficiency of microwave generation; in fact, defining  $\eta_e = P/(VI_r)$ , where  $I_r$  is the radial portion of the total current  $I = I_r + I_z$ , and  $I_z$  is the axial portion of the current, we can easily show that (see Problem 13)

$$\eta_\mu = \eta_e \left( \frac{I_r}{I} \right) \quad (7.22)$$

Now, axial current flow arises from parasitic losses off the end of the cathode and from axial drifts that flush electrons from the interaction region. Unfortunately, this loss mechanism is self-enhancing, since axial currents increase the azimuthal component of the magnetic field, which in concert with the radial electric field increases the axial  $E_r \times B_\theta$  drift of electrons out of the interaction region. The enhanced drop in output power with axial current flow is shown in Figure 7.30.<sup>17</sup> Research into the use of end caps, which in reality are rounded, as shown in Figure 7.16, to reduce the electric fields and corresponding field emission losses there, has minimized parasitic end losses from the end of the cathode. Nevertheless, the intrinsically high operating currents of relativistic magnetrons will always create some  $B_\theta$  and resulting axial electron loss.

Inverted magnetrons, with the anode on the inside and the cathode on the outside, eliminate the energy loss due to axial current flow because the axially

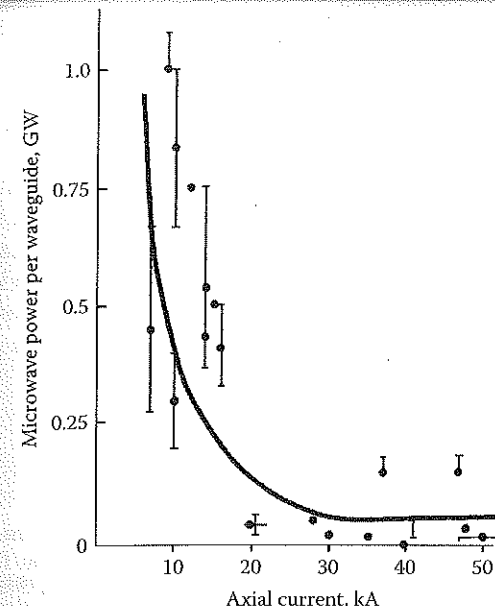


FIGURE 7.30

Reduction in power with increasing axial current loss. (From Benford, J. et al., *IEEE Trans. Plasma Sci.*, PS-13, 538, 1985. With permission.)

flowing electrons return to the cathode. Inverted magnetrons were originally studied at MIT,<sup>32</sup> Stanford,<sup>29</sup> and NRL.<sup>51</sup> In general, all groups reported an overall reduction in output power. The MIT group proposed that their radial extraction method, which required extracted radiation to propagate through the electron space-charge layer, fundamentally limited the efficiency. Ballard proposed that the inverted resonator does not generate RF fields as high as in the normal geometry.<sup>52</sup> The Tomsk group, observing that the length of a voltage pulse in a coaxial diode with inverted polarity is three to four times that of an ordinary diode at equal electric fields, operated an inverted magnetron for almost the entire pulse length of the applied voltage<sup>53</sup> (Figure 7.31). During the 900-nsec pulse, unfortunately the magnetron moved from one mode to another as the voltage changed, in a manner consistent with gap closure. A frequency variation of 30% during the pulse was reported. Consequently, this experiment, although producing the longest pulse yet observed, points to the problematic relationship between impedance and voltage control in high power devices and long-pulse, single-frequency operation.

Efficiency, particularly the efficiency of microwave generation,  $\eta_\mu$ , and its electronic component  $\eta_e$ , is an important factor in device lifetime. Electron kinetic energy not converted into microwave energy by electrons crossing the gap is deposited in the anode. In contrast to the conventional magnetron, the relativistic magnetron's high-voltage electrons have penetration depths of a few millimeters. Damage occurs in the interior of the vanes and the cathode